

Transport processes and dynamics in chemical reaction models and in oceanic models.

**Makrina Agaoglou**

Universidade Federal da Bahia  
makrina.agaoglou@upm.es



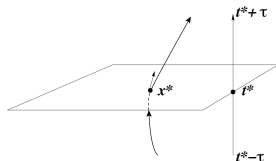
- 1 Theoretical part and main ideas
  - Phase space
  - Langrangian Descriptors
  - Chemical Reaction Dynamics
- 2 First Example (Chemical Reaction Dynamics)
- 3 Second Example (Oceanic modeling)
- 4 Third Example (Oceanic modeling)

- Phase space structures are a geometrical way to look into the solutions of systems of differential equations.
- This geometrical approach allows to recognize at a glance regions into the phase space with distinct origins or fates.
- This geometrical approach has an impact on the understanding of transport in chemical reaction dynamics/geophysical flows.

# Langragian Descriptors

We obtain the phase space structures using the method of Lagrangian Descriptors that is based on the function  $M$ .

The function  $M$  measures the length of the trajectory curve projected on the phase space when it is evolved forward and backward in time a  $\tau$  interval.



## Original Method-Arclength Definition (Madrid & Mancho 2009)

Scalar function measuring trajectory arclength starting at an initial condition  $x_0 = x(t_0)$  as it evolves forward/backward for a time  $\tau$ .

$$M(x_0, t(0), \tau) = \int_{t_0-\tau}^{t_0+\tau} \|v(x(t; x_0), t)\| dt = M^{(f)} + M^{(b)}$$

## Lagrangian Descriptors (p-norm Definition), $p \in (0, 1]$

$$M_p(x_0, t_0, \tau) = \int_{t_0-\tau}^{t_0+\tau} \sum_{i=1}^N |\dot{x}_i(t; x_0)|^p dt = M_p^{(f)} + M_p^{(b)}$$

Mathematical analysis of **singular structures** (non-differentiability and relationship between LDs and **invariant manifolds**)

# Chemical Reaction Dynamics

## Transition State Theory (1930s)- Determine Chemical Reaction Rates

- Eyring, Polanyi and others - (Thermodynamics)
- Wigner, "Phase space is the arena for chemical reactions"

## Goal

Search for Dividing Surface (DS) in phase space separating reactants from products with minimal flux and no-recrossing properties

**Flux across the dividing surface = chemical reaction rate**

## Lyapunov Subcenter Manifold Theorem

Normally Hyperbolic Invariant Manifolds (NHIMs) bifurcating from index-1 saddles provide scaffolding to construct the DS

# First Example (Chemical Reaction Dynamics)

Joint work with

- Stephen Wiggins (University of Bristol, UK)
- Victor Garcia Garrido (University of Alcala, Spain).

## Example: 4 well potential

The **Hamiltonian**:

$$H(x, y, p_x, p_y) = \frac{1}{2} p_x^2 + \frac{1}{2} p_y^2 + V(x, y), \quad (1)$$

where the mass in each DoF is  $m_x = m_y = 1$ ,  $\delta$  is the model parameter representing the asymmetry in the double well potential of the  $x$  DoF,  $\alpha$  measures the barrier height corresponding to the potential of the  $x$  DoF, and  $\beta$  represents the coupling strength between both DoF in the system.

The **PES**:

$$V(x, y) = x^4 - \alpha x^2 - \delta x + y^4 - y^2 + \beta x^2 y^2. \quad (2)$$



The dynamical evolution of the Hamiltonian system in Eq. (1) takes place in a four-dimensional phase space, and is determined by Hamilton's equations of motion:

$$\left\{ \begin{array}{l} \dot{x} = \frac{\partial H}{\partial p_x} = p_x \\ \dot{y} = \frac{\partial H}{\partial p_y} = p_y \\ \dot{p}_x = -\frac{\partial H}{\partial x} = -\frac{\partial V}{\partial x} = -4x^3 + 2\alpha x + \delta - 2\beta xy^2 \\ \dot{p}_y = -\frac{\partial H}{\partial y} = -\frac{\partial V}{\partial y} = -4y^3 + 2y - 2\beta x^2 y \end{array} \right. \quad (3)$$

Consider the symmetric and uncoupled system with energy  $H_0$ . Since the system is conservative, dynamics is constrained to the three-dimensional energy hypersurface:

$$\mathcal{S}(H_0) = \left\{ (x, y, p_x, p_y) \in \mathbb{R}^4 \mid H_0 = \frac{1}{2} (p_x^2 + p_y^2) + x^4 - x^2 + y^4 - y^2 \right\}, \quad (4)$$

and the total energy of the system can be split between both DoF to yield:

$$H(x, y, p_x, p_y) = H_x(x, p_x) + H_y(y, p_y), \quad (5)$$

# PES for the uncoupled and symmetric H.S.

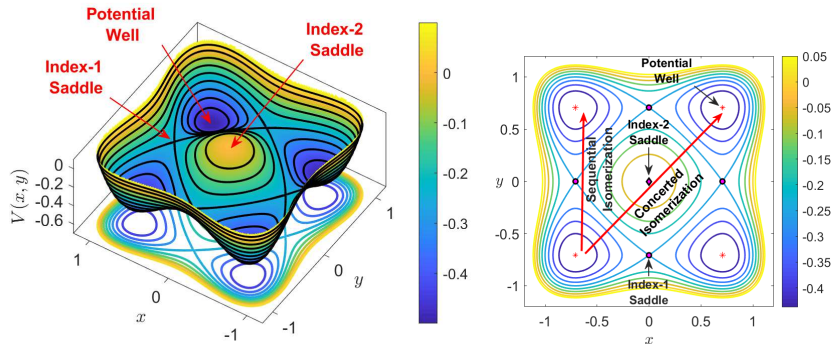
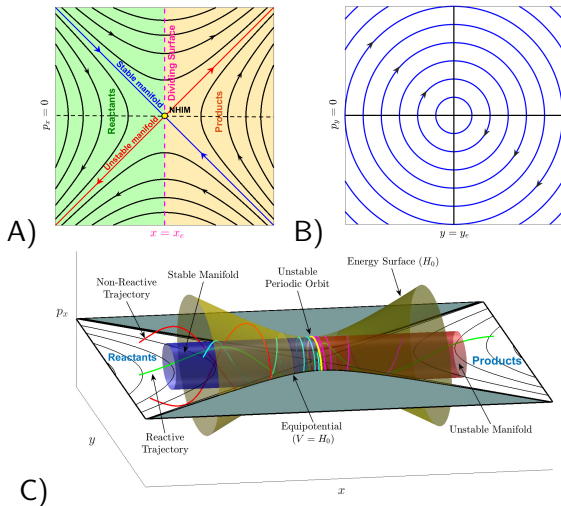


Figure: Potential energy surface in Eq. (2) for the uncoupled ( $\beta = 0$ ) and symmetric ( $\delta = 0$ ) Hamiltonian system.



**Figure:** Phase space structures of the linearized Hamiltonian given in the neighborhood of the index-1 saddle  $\mathbf{x}_e = (0, \sqrt{2}/2, 0, 0)$ . Panel A) depicts the saddle space, B) is the center space, and C) represents the phase space bottleneck in the vicinity of the index-1 saddle that allows transport, i.e. reaction, from reactants to products.

## Goal

Our **goal** is to analyze, in terms of the model parameters, the geometrical template of phase space structures, i.e. the underlying isomerization pathways, that characterizes the dynamical behavior of the system.

## Method

By applying the method of Lagrangian descriptors (LDs)

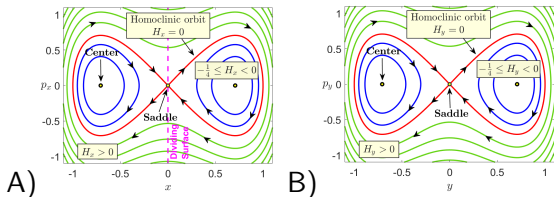


**Figure:** For the symmetric and uncoupled Hamiltonian system with energy  $H_0 = -0.15$  in the neighborhood of the equilibrium point  $\mathbf{x}_e = (0, \sqrt{2}/2, 0, 0)$ . A) and B) depict the phase portraits in the  $x - p_x$  and  $y - p_y$  planes respectively. We have marked with a magenta line the dividing surface  $x = 0$  that separates the upper-left and upper-right wells of the PES.

For our analysis of the system, we fix a total energy of  $H_0$  and consider a phase space slice that goes through the lower index-1 saddle of the PES:

$$\mathcal{P}_1 = \left\{ (x, y, p_x, p_y) \in \mathbb{R}^4 \mid y = -1/\sqrt{2}, p_y > 0 \right\}, \quad (6)$$

and another Poincaré surface of section (PSOS) that coincides with the configuration plane:

$$\mathcal{P}_2 = \left\{ (x, y, p_x, p_y) \in \mathbb{R}^4 \mid p_x = 0, p_y > 0 \right\}. \quad (7)$$

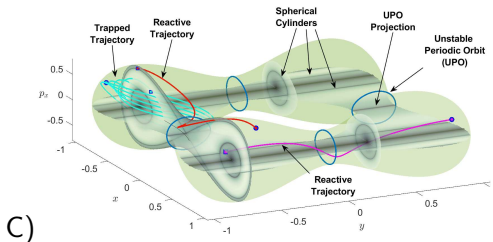
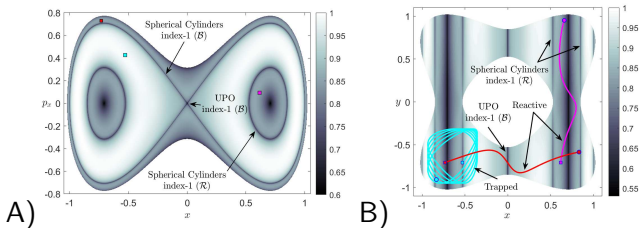


**Figure:** Phase space structures and evolution of initial conditions at  $H_0 = -0.2$ . A) LDs calculated using  $\tau = 5$  on the phase space slice in Eq. (6). B) Superposition of LDs calculated using  $\tau = 5$  on the PSOS in Eq. (7) with the dynamical evolution of the initial conditions selected in panel A. C) Visualization of the phase space dynamics in the 3D energy hypersurface.



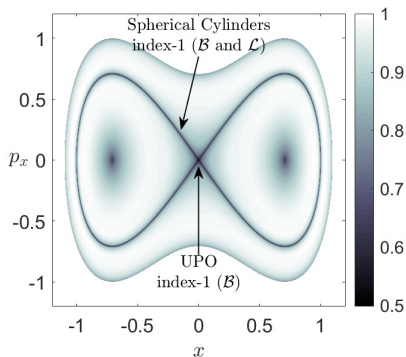


**Figure:** Phase space structure at energy  $H_0 = 0$  for the symmetric and uncoupled Hamiltonian, as revealed by Lagrangian descriptors using  $\tau = 5$  on the PSOS in Eq. (6).

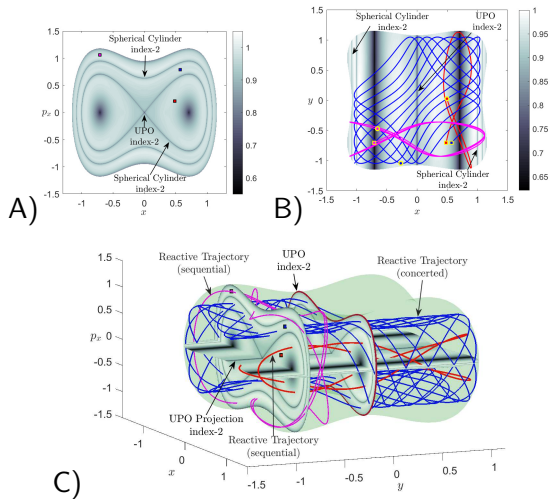


**Figure:** Phase space structures and evolution of initial conditions at  $H_0 = 0.2$ . A) LDs calculated using  $\tau = 5$  on the phase space slice in Eq. (6). B) Superposition of LDs calculated using  $\tau = 5$  on the PSOS in Eq. (7) with the dynamical evolution of the initial conditions selected in panel A. C) Visualization of the phase space dynamics in the 3D energy hypersurface.

# Asymmetric Case

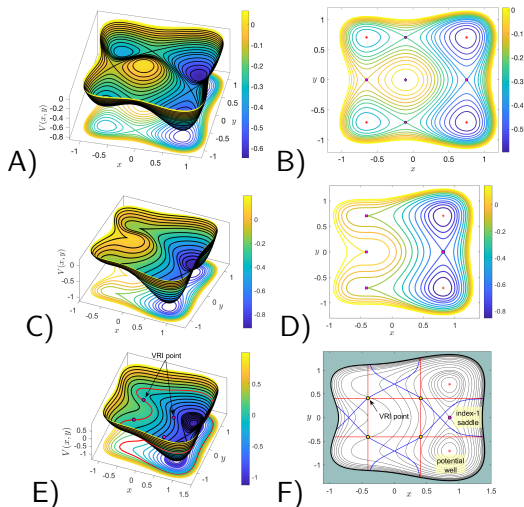


Figure: Potential energy surface landscape (left column) and equipotential curves in configuration space (right column)

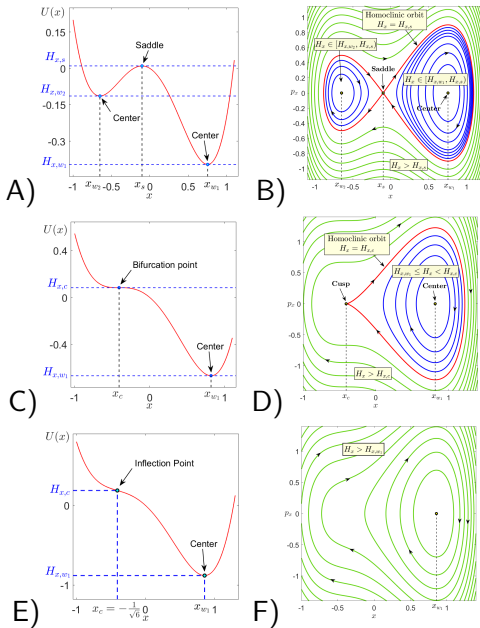
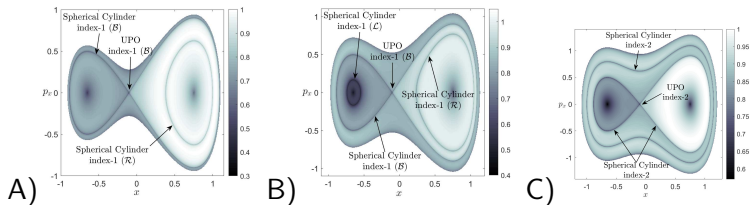
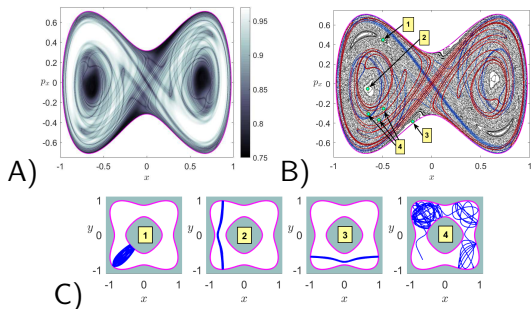


Figure: Potential energy for the  $x$  DoF and associated  $x$ - $p_x$  phase portrait.




**Figure:** Lagrangian descriptors calculated using  $p = 1/2$  and  $\tau = 5$  on the surface of section  $y = -\sqrt{2}/2$  for the asymmetric uncoupled Hamiltonian system with  $\delta = 0.2$ . Energy levels: A)  $H_0 = -0.2$ , which is below the energy of the left index-1 saddle and above that of the bottom index-1 saddle; B)  $H_0 = -0.1$ , that is above the energy of the left index-1 saddle and below that of the index-2 saddle; C)  $H_0 = 0.2$ , above the energy of the index-2 saddle.

# Coupled Case



**Figure:** Phase space structures on the surface of section given in Eq. (6) at an energy  $H_0 = -0.2$  and dynamical evolution of initial conditions for the symmetric and coupled Hamiltonian with  $\alpha = 1$ ,  $\delta = 0$  and  $\beta = 0.2$ . A) LDs calculated using  $p = 1/2$  and  $\tau = 12$ . B) Poincaré map superimposed with the stable (blue) and unstable (red) manifolds extracted from the gradient of the LD function. We have also marked in the picture four different types of initial conditions. C) Dynamical evolution of the initial conditions selected in panel B). In all diagrams we have indicated the energy boundary with a magenta curve.

-  Exploring Isomerization Dynamics on a Potential Energy Surface with an Index-2 Saddle using Lagrangian Descriptors”, V. J. García Garrido, M. Agaoglou, S. Wiggins, Communications in Nonlinear Science and Numerical Simulation, Vol. 89, (2020)



## Second Example (Oceanic modeling)

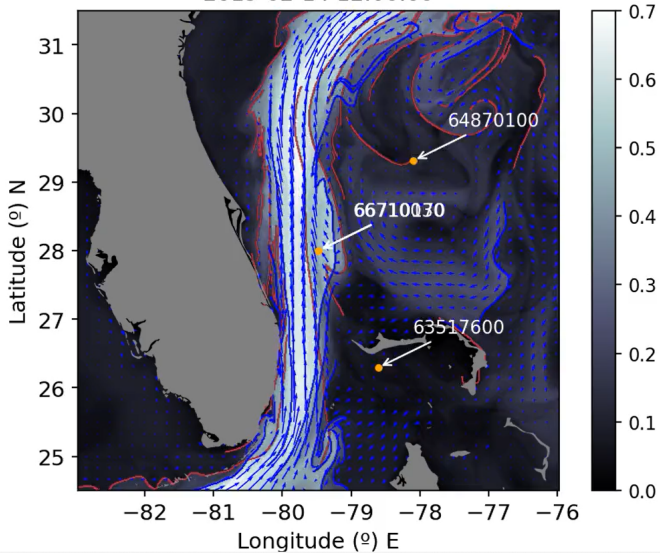
joint work with

- Guillermo García-Sánchez (CTO of Digital Earth Solutions)
- Evanne Marie Claire Smith (University of Bologna)
- Ana M. Mancho (ICMAT, CSIC)

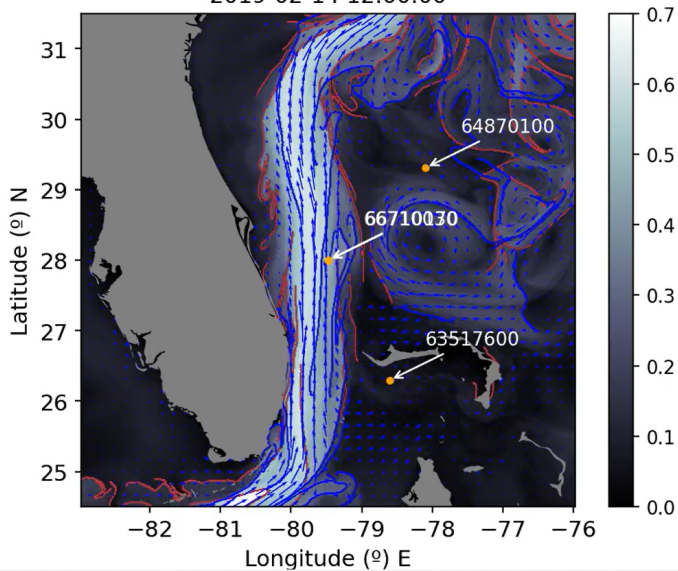


- Comparison of the transport performance of the analysis and reanalysis ocean models against observed drifters in a specific domain in the North Atlantic
  - qualitative (LDs)
  - quantitative (LUQ)

2019-02-14 12:00:00



2019-02-14 12:00:00





Contents lists available at [ScienceDirect](#)

## Commun Nonlinear Sci Numer Simulat

journal homepage: [www.elsevier.com/locate/cnsns](http://www.elsevier.com/locate/cnsns)



### A bridge between invariant dynamical structures and uncertainty quantification

G. García-Sánchez<sup>a</sup>, A.M. Mancho<sup>a,\*</sup>, S. Wiggins<sup>b</sup>

<sup>a</sup> Instituto de Ciencias Matemáticas, CSIC, C/Nicolás Cabrera 15, Campus Cantoblanco, Madrid 28049, Spain

<sup>b</sup> School of Mathematics, Fry Building, Woodland Road, University of Bristol, Bristol BS8 1UG, United Kingdom



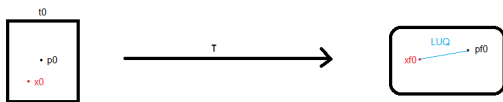
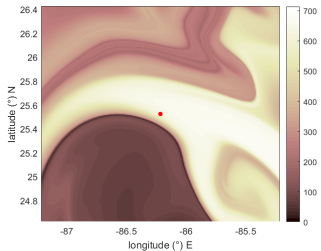
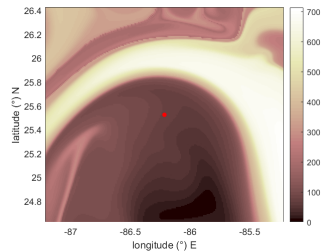


Figure: LUQ method

$$LUQ(t = t_0) = \|x(t_0 + \tau) - p(t_0 + \tau)\| = \|x_{f_0} - p_{f_0}\| \quad (8)$$

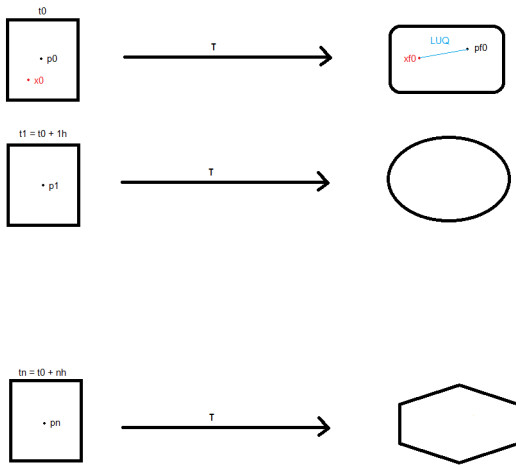


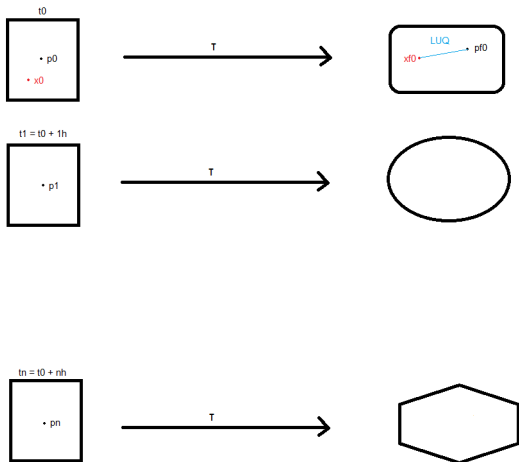
a)



b)

Figure: LUQ method





$$norm = \max |p_i - p_j|, \text{ where } i, j = 1, \dots, n \text{ and } i \neq j \quad (9)$$



	$\tau = 5$	$\tau = 10$	$\tau = 15$
Radius=10	0.43333	0.61883	0.89682
Radius=30	0.52146	0.65785	0.82414
Radius=60	0.6871	0.80307	0.96242

	$\tau = 5$	$\tau = 10$	$\tau = 15$
Radius=10	0.46714	0.6646	0.93635
Radius=30	0.54436	0.6729	0.88899
Radius=60	0.71181	0.81433	0.98547

	$\tau = 5$	$\tau = 10$	$\tau = 15$
Radius=10	-0.033812	-0.045768	-0.039527
Radius=30	-0.022893	-0.015058	-0.064845
Radius=60	-0.024713	-0.01126	-0.023045

**Table:** Exp 1, Top table is analysis, middle table reanalysis, bottom table difference analysis-reanalysis,  $t_0 = 03/02/2019$  12:00:00 over 22 days, norm max = 77.2317 km

	$\tau = 5$	$\tau = 10$	$\tau = 15$
Radius=10	0.14123	0.23417	0.33554
Radius=30	0.15095	0.23654	0.34365
Radius=60	0.17401	0.262	0.36967

	$\tau = 5$	$\tau = 10$	$\tau = 15$
Radius=10	0.18467	0.26019	0.31986
Radius=30	0.18633	0.25373	0.31597
Radius=60	0.20849	0.27406	0.3537

	$\tau = 5$	$\tau = 10$	$\tau = 15$
Radius=10	-0.043438	-0.026019	0.015683
Radius=30	-0.035388	-0.017199	0.027678
Radius=60	-0.034481	-0.012063	0.015971

**Table:** Exp 2, Top table is analysis, middle table reanalysis, bottom table difference analysis-reanalysis,  $t_0 = 13/02/2019$  12:00:00 over 22 days, norm max = 709.5687 km

	$\tau = 5$	$\tau = 10$	$\tau = 15$
Radius=10	0.47622	0.81484	1.0064
Radius=30	0.48378	0.85589	1.0822
Radius=60	0.50075	0.88593	1.1474
Radius=100	0.6013	0.98987	1.2466

	$\tau = 5$	$\tau = 10$	$\tau = 15$
Radius=10	0.15794	0.2011	0.14646
Radius=30	0.19921	0.27238	0.23547
Radius=60	0.32352	0.51573	0.58798
Radius=100	0.51583	0.7634	0.89678

	$\tau = 5$	$\tau = 10$	$\tau = 15$
Radius=10	0.31828	0.61374	0.85992
Radius=30	0.28458	0.58351	0.84673
Radius=60	0.17723	0.3702	0.55939
Radius=100	0.085473	0.22646	0.34986

**Table:** Exp 3, Top table is analysis, middle table reanalysis, bottom table difference analysis-reanalysis,  $t_0 = 22/01/2019$  12:00:00 over 22 days, norm max

While reanalysis tends to perform better in some cases also analysis is performing very well.

# Third example: New links between invariant dynamical structures and uncertainty quantification

Joint work with

- Stephen Wiggins (University of Bristol, UK)
- Ana Maria Mancho (ICMAT, CSIC, Spain)
- Guillermo García-Sánchez (CTO of Digital Earth Solutions)

## Second example: New links between invariant dynamical structures and uncertainty quantification

- With this example we propose a new uncertainty measure, appropriate for quantifying the performance of transport models in assessing the origin or source of a given observation.
- It is found that in a neighbourhood of the observation the proposed uncertainty measure is related to the invariant dynamical structures of the model.

# Uncertainty Quantification in Backward Time

Our interest is in quantifying the uncertainty of a model for identifying a target source  $\mathbf{x}^*$ , which is consistent with a later observation  $\mathbf{x}_1$  at time  $t_1$ . In this way, the target source,  $\mathbf{x}^*$ , is located at an earlier time  $t^* = t_1 - \tau$ .

$$L_{BUQ}(\mathbf{X}_1, t_1, \tau, p) = \sum_{i=1}^n |x_i(t_1 - \tau) - x_i^*|^p, \quad p \leq 1, \quad \mathbf{X}_0 \in \mathbb{R}^n, \tau > 0. \quad (10)$$

where  $\mathbf{X}_1$  represents a neighbourhood around the observation  $\mathbf{x}_1 = (x_1, x_2, \dots, x_n)$  at time  $t_1$  being  $n$  the dimension of the dynamical system, which in our specific examples is  $n = 2$ . The coordinates of the target are  $(x_1^*, x_2^*)$ , and uncertainty is provided in terms of a distance metric between the target and the *backward* evolution of points near to  $\mathbf{x}_1$  for a period  $\tau$ .

Simulations has demonstrated that the spill was closely following fluid parcel trajectories  $x(t)$  that obeyed the equation:

$$\begin{aligned}\frac{d\lambda}{dt} &= \frac{u(\lambda, \phi, t)}{R \cos \phi} \\ \frac{d\phi}{dt} &= \frac{v(\lambda, \phi, t)}{R}\end{aligned}$$

where the position of the fluid parcel at the ocean surface is given in longitude ( $\lambda$ ) and latitude ( $\phi$ ), and  $R$  is the Earth's radius. These  $u, v$  velocity components are obtained as data sets from the Copernicus Marine Monitoring Environmental Service (CMEMS).



Models such as that given in the previous equations, possess a transport signature based on invariant manifolds associated with hyperbolic trajectories, which following Poincaré's idea. These geometrical features allow a more robust analysis of the transport capacity of ocean currents than that based on individual trajectories.

Models such as that given in the previous equations, possess a transport signature based on invariant manifolds associated with hyperbolic trajectories, which following Poincaré's idea. These geometrical features allow a more robust analysis of the transport capacity of ocean currents than that based on individual trajectories.

In the context of geophysical flows, these geometrical structures are referred to as Lagrangian Coherent Structures (LCSs). The use of LCS allows a qualitative assessment of the performance of data sets, however, definitions such as that BLUQ allow a quantitative analysis that we will implement next in the context of the oil spill event described in. In this work, we compute LCS using Lagrangian Descriptors.

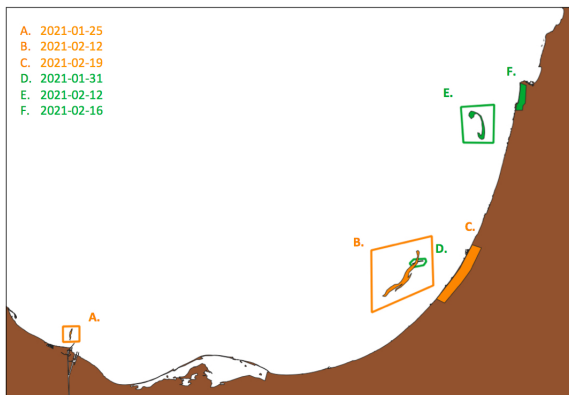


**Figure:** A graphical representation of the spills observed along the coastline of the Eastern Mediterranean and satellite observations matching the sources.

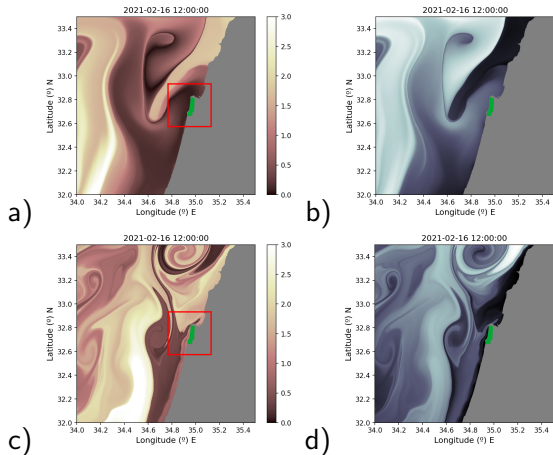


**Figure:** Evaluation on the 16th of February 2021 of  $L_{BUQ}$  using the target,  $\mathbf{x}^* = (34.36^\circ\text{E}, 31.78^\circ\text{N})$  and of  $M^{(b)}$  using  $\tau = 16$  days; a)  $L_{BUQ}$  with the CMEMS global product; b)  $M^{(b)}$  with the CMEMS global product; c)  $L_{BUQ}$  with the CMEMS Mediterranean product; d)  $M^{(b)}$  with the CMEMS Mediterranean product.

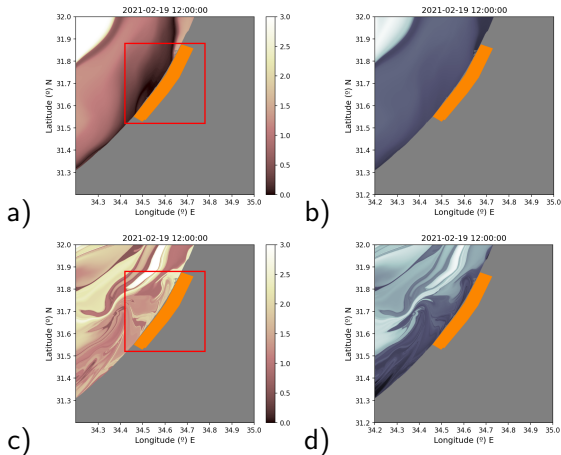


**Figure:** Evaluation on the 19th of February 2021 of  $L_{BUQ}$  using the target,  $\mathbf{x}^* = (34.32^\circ\text{E}, 31.35^\circ\text{N})$  and of  $M^{(b)}$  using  $\tau = 25$  days; a)  $L_{BUQ}$  with the CMEMS global product; b)  $M^{(b)}$  with the CMEMS global product; c)  $L_{BUQ}$  with the CMEMS Mediterranean product; d)  $M^b$  with the CMEMS Mediterranean product.

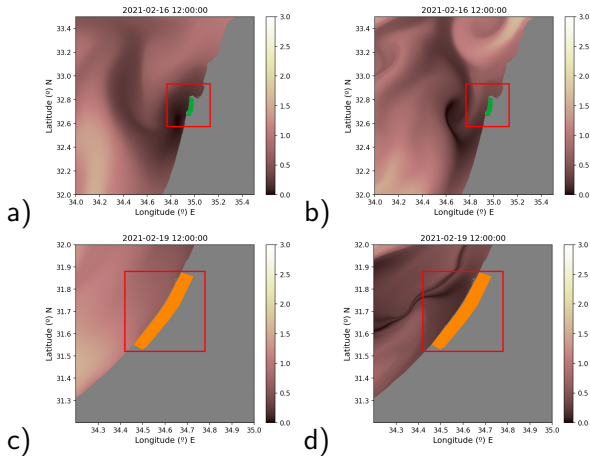


**Figure:** Evaluation  $L_{BUQ}$  on the Israel and Gaza coast for the close targets using the global and the Mediterranean data. a)  $L_{BUQ}$  on 16th of February 2021 using the target,  $\mathbf{x}^* = (34.32^{\circ}\text{E}, 31.35^{\circ}\text{N})$  on the CMEMS global product; a)  $L_{BUQ}$  with the CMEMS global product; b)  $M^{(b)}$  with the CMEMS Mediterranean product; c)  $L_{BUQ}$  with the CMEMS global product; d)  $M^{(b)}$  with the CMEMS Mediterranean product.

# Conclusions

- We have found that the defined quantity  $L_{BUQ}$ , when evaluated in the neighborhood of an observation with respect to its backward-in-time target, has a structure which has been linked to the unstable invariant manifolds of the hyperbolic trajectories present in the model vector field. This link has been rigorously proven in a simple example, and numerically verified in a real inspired case: the oil spill accident that affected the Eastern Mediterranean in 2021.
- The new definition,  $L_{BUQ}$ , has been exploited to quantify the performance of different CMEMS products to describe the sequence of events regarding the oil spill accident in the Eastern Mediterranean in 2021. In this event, some of the backward-in-time targets are very far from the impact point, and their evolution involves mesoscale structures, which our analysis shows are better represented in the CMEMS global model. On the contrary for targets that are close, involving submesoscale structures, on average the CMEMS Mediterranean product performs better, although in some cases CMEMS global product also performs well.



New links between invariant dynamical structures and uncertainty quantification, G. García Sánchez, A. M. Mancho, M. Agaoglou, S. Wiggins, *Physica D: Nonlinear Phenomena*, Vol. 453, (2023)



**Acknowledgments** MA acknowledges support by the Society of Spanish Researchers in Southern Africa (ACE Sur de Africa), through the grant for FRA Visiting Lecturers Grants Program that they are sponsored by the Ramón Areces Foundation (FRA) and the Embassies of Spain in Angola, Mozambique, South Africa and Zimbabwe.



Thank you!



makrina.agaoglou@upm.es



<https://makrinaagaoglou.wordpress.com/>